CORA Cork Open Research Archive
Cartlann Taighde Oscailte Chorcaí

Title	Morphological evolution of lamellar forming polystyrene-block-poly(4-vinylpyridine) copolymer under solvent annealing
Authors	Ghoshal, Tandra;Chaudhari, Atul;Cummins, Cian;Shaw, Matthew T.;Holmes, Justin D.;Morris, Michael A.
Publication date	2016-05-17
Original Citation	Ghoshal, T., Chaudhari, A., Cummins, C., Shaw, M. T., Holmes, J. D. and Morris, M. A. (2016) 'Morphological evolution of lamellar forming polystyrene-block-poly(4-vinylpyridine) copolymers under solvent annealing', Soft Matter, 12(24), pp. 5429-5437. doi: 10.1039/c6sm00815a
Type of publication	Article (peer-reviewed)
Link to publisher's version	http://pubs.rsc.org/en/journals/journalissues/sm#!recentarticles&adv - 10.1039/c6sm00815a
Rights	© The Royal Society of Chemistry 2016
Download date	2026-11-15 14:05:24
Item downloaded from	https://hdl.handle.net/10468/6754

UCC
University College Cork, Ireland
Coláiste na hOllscoile Corcaigh

Morphological evolution of lamellar forming polystyrene-*block*-poly(4-vinylpyridine) copolymer under solvent annealing

Tandra Ghoshal,[1,2*] Atul Chaudhari,[1,2] Cian Cummins,[2] Matthew T. Shaw,[3] Justin D. Holmes,[1,2] Michael A. Morris[2*]

[1]Department of Chemistry and Tyndall National Institute, University College Cork, Cork, Ireland

[2]AMBER, Centre for Research on Adaptive Nanostructures and Nanodevices (CRANN), Trinity College Dublin, Dublin, Ireland.

[3]Intel Ireland Ltd., Collinstown Industrial Estate, Co. Kildare, Ireland

[*] Corresponding Author:

Prof. Michael A. Morris

Tel: +353 1 896 3089

Fax: +353 1 896 3089

E-mail: morrism2@tcd.ie

And

Tandra Ghoshal

Tel: + 353 21 490 2911

Fax: +353 21 427 4097

E-mail: g_tandra@yahoo.co.in

In this work, we are reporting a very simple and efficient method to form lamellar structures of symmetric polystyrene-*block*-poly(4-vinylpyridine) (PS-*b*-P4VP) copolymer thin films with vertically (to the surface plane) orientated lamellae using a solvent annealing approach. The methodology does not require any brush chemistry to engineer a neutral surface and it is the block neutral nature of the film-solvent vapour interface that defines the orientation of the lamellae. The microphase separated structure of two different molecular weight lamellar forming PS-*block*-P4VP copolymer formed under solvent vapour annealing was monitored using atomic force microscopy (AFM) so as to understand morphological changes of the films under different solvent exposure. In particular, the morphology changes from micellar structures to well-defined microphase separated arrangements. The choice of solvent/s (single and dual solvent exposure) and the solvent annealing conditions (temperature, time etc.) had important effects on structural transitions of the films and it was found that a block neutral solvent was required to realize vertically aligned P4VP lamellae. The results of structural variation of the phase separated nanostructured films through the exposure to ethanol are also described.

Introduction

Block copolymers (BCPs) of two or more chemically immiscible polymer chains can phase separate to form well-ordered morphologies with feature sizes of around 5 to 50 nm in thin films under certain conditions.[1] BCPs may be one of the most useful classes of nanomaterials because of their ability to self-assemble into different morphologies and subsequently template organic, inorganic, semiconducting, metallic or biologically relevant material nanopatterns.[2-11] BCP self-assembled structures can form are lamellar, cylindrical, spherical as well as more complex gyroid and other 3D arrangements depending on their composition. The feature sizes and lateral spacing of the patterns varies with molecular weight. The Flory-Huggins interaction parameter (χ), a measure of block chemical dissimilarity, combined with the degree of polymerization (N) dictates [12-13] the spontaneous formation of microphase separated structure.[14-15] Spin-coating from dilute polymeric solution onto flat substrates is the most convenient method of thin film formation but the as-spun films are usually in a non-equilibrium state due to the competition between microphase separation and vitrification as solvent evaporation proceeds.[16] Self-assembly of BCPs can be achieved through annealing the BCP thin film under a suitable environment, either at elevated temperature using thermal annealing[17-18] or by annealing under solvent vapour/s[19-25]. Of particular interest here is solvent vapour annealing (SVA) since well-defined film patterns can be achieved at much lower process temperatures/times than thermal annealing. In solvent annealing, the solvent vapour permeates, swells and separates the polymer chains providing mobility by lowering the effective glass transition temperature.

Because of their potential as an "on-chip" etch mask in integrated circuit manufacture, orientational control (i.e. direction vertical or parallel to the substrate plane) is a critical issue.[26-27] This can be challenging particularly for lamellar systems where preferential interface

interactions and surface energies can result in horizontal orientations and/or preferential wetting layers.[28] Examples include polystyrene-*block*-polymethylmethacrylate (PS-*block*-PMMA) which is well studied for device applications but requires a well-defined random polymer brush layer on top of the silicon substrate to provide ideally oriented patterns.[29] Polystyrene-*block*-polydimethlysiloxane (PS-*block*-PDMS) is another potential material for circuit fabrication but also requires a carefully controlled brush layer or substrate molecular functionalization.[30] Other potential solutions include "capping layers" but a simple method was first demonstrated by Libera and co-workers[31], who proposed that solvent evaporation upon casting could orient cylinder during solvent evaporation. However, this mechanism is not clear and other authors suggest that the chemistry of the solvent vapour at the polymer surface drives orientational control.[25]

An ideal line-forming BCP pattern for circuit fabrication would be lamellar-forming (since pattern transfer from cylindrical arrangements is challenging[27]) and have high χ (since they can phase separate into small domain size/spacings, have smaller inter-domain diffusion regions and produce patterns with less defects). The use of high-χ BCPs is, however, challenging since it is difficult to ensure perpendicular orientation of the blocks to the substrate plane and, further, obtaining well-ordered, defect free patterns can be kinetically slow.[32] At room temperature, the χ parameter of PS-*block*-P4VP (χ~0.34)[33] is considerably higher than those of PS- *block*-PDMS (χ~0.26),[34] PS-*block*-PMMA (χ~0.06),[35] PS-*block*-P2VP (χ~0.18),[36] PS-*block*-PEO (χ~0.08).[37] Further, the surface energies of PS and P4VP are similar limiting phase separation at interfaces[38] whilst the functionality of the block is ideal for inclusion of inorganics for enhancement of etch contrast. Thus, the PS-*block*-P4VP system has significant potential in device fabrication. However, the self-assembly of lamellar forming systems of this BCP is challenging due to a

strong tendency to micellization in common polymer solvents such as toluene.[39] Indeed, this strong micellization has been used for the incorporation of metals and semi-conducting materials into the P4VP core in solvents favouring PS.[40-41] Sohn and co-workers[42] have shown long range lateral ordering of PS-*b*-P4VP micelles is possible. Generally, the micelles formed by lamellar PS-*block*-P4VP are robust and resistant to both thermal and solvent annealing and in order to form microphase separated domain structures, although careful attention to the selection of both casting and annealing solvents are required.[16]

SVA methodologies are well developed. This paper extends the understanding of SVA by extension to a high-χ lamellar phase BCP which shows very strong tendency to form micelles in both solution and thin films and provides details of a robust solvent annealing method to form periodic, orientationally controlled, lamellar structures and provide understanding of the nature of the SVA solvent needed to affect these arrangements.

Experimental Section

Two different PS-*block*-P4VP copolymers were purchased from Polymer Source Inc. (Montreal, Canada). Table 1 shows the molecular characteristics of the polymers used in this work. BCPs were used without any further purification. Reagent grade toluene and tetrahydrofuran (THF) were purchased from Sigma-Aldrich.

Table 1: Molecular characteristics of the PS-*block*-P4VP copolymers

Polymer	Total M_n (x10^3 g/mol)	M_w/M_n (PDI)	P4VP Fraction	BCP morphology(*)
PS_{20k}-*block*-$P4VP_{17k}$	37.0	1.08	0.46	L
PS_{9k}-*block*-$P4VP_{9.2k}$	18.2	1.09	0.51	L

* L= Lamellae forming

Polymers used were generally dissolved in toluene-THF mixtures to yield 0.5 weight % solutions and were stirred overnight at room temperature to ensure complete solution. A toluene-THF

(80%-20%) mixture was found to be the optimum composition providing periodic arrangements in short times (see below). Substrates were silicon (100) wafers with an interfacial oxide of 2 nm and were cleaned by sonicating for 15 min in toluene, followed by 10 min in THF and then dried under a stream of nitrogen. A final cleaning using a UV/ozone treatment for 15 min was performed. The cleaning procedure lowered the water contact angle significantly (36^{o} for bare silicon and 0^{o} for UV/ozone cleaned) making the surface more hydrophilic. This resulted in a more uniform, high coverage thin film presumably due to increased affinity to the P4VP block. Thin films of required thickness were prepared by spin-coating the polymer solutions onto the substrates at 3000 rpm for 30 s using a Speciality Coating Systems G3P-8 spin-coater. Solvent annealing was used to generate well-defined periodic structures. The samples were placed in a glass bottle (100 ml size) containing a smaller vial holding 10 ml of solvent. As cast samples were then solvent annealed at 50 ^{o}C for a range of different times (30 min to 6 h). The annealed samples were immediately removed from the vials and kept at room temperature for few minutes to ensure the rapid and complete evaporation of the solvent. The rapid removal time was used so that swollen features were kinetically "frozen-in" for analysis. All samples were analysed using atomic force microscopy (AFM, Park Systems XE-100) and topographic images were collected in non-contact tapping mode. Scanning electron microscopy (SEM, FEI Inspect F) was also used as an imaging method.

Results

A 0.5 wt% solution used here for spin casting is well above the known critical micelle solution for PS_{20k}-*block*-$P4VP_{17k}$ (0.065 mg ml^{-1}) copolymer and strong spherical micellization is expected when dissolved in toluene.[43] Because of the preferential interaction of toluene with the PS block the micelles have a PS corona and the P4VP block in the core.[44] When the casting

solution is spin-coated on the substrate surface, these micelles survive spin coating/solvent evaporation and in the conditions used here, form a monolayer of densely packed, robust hemi-micelles on the substrate surface and form a poorly ordered hexagonal arrangement (Fig. 1(A)). In the AFM image, lighter colours correspond to the P4VP block and the darker colour to PS. The formation of strong spherical micellization in these mixtures is observed by the bluish translucent colour of the polymer solution.[45] Below, 0.5 wt% casting solution concentrations, the micelles become progressively less densely packed and it is possible to resolve the micelle structure using SEM (0.3 wt%). In Fig. 1(B), the micelles do not cover the whole surface and open areas of the substrate can be seen. At higher resolution, Fig. 1(C), a densely packed P4VP core can be clearly observed as a bright sphere with the less densely packed PS corona seen as tendrils extending across the substrate. It can be seen that the PS component has collapsed to the substrate either the result of surface interactions and/or the removal of the solvent.

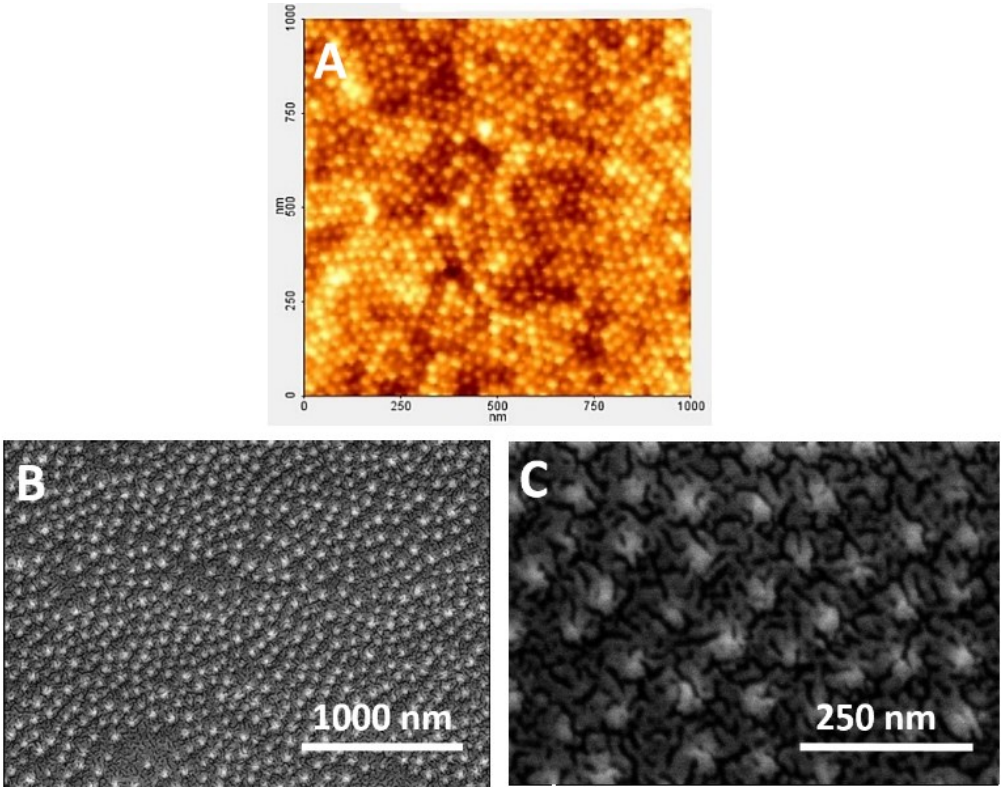


Fig. 1 AFM images of a PS_{20k}-*block*-$P4VP_{17k}$ copolymer thin films, 0.5 wt% casting solution (A). (B) and (C) are SEM images of similar films formed at 0.3 wt%. The micelle nature of the film can be very clearly seen in (C).

In order to rearrange these films into microphase separated structures, extensive annealing was needed. Thermal annealing was not very effective and instead solvent annealing was found to be much more effective. As discussed by us previously,[16] the choice of solvent is dictated by the materials solvent parameter. For these strongly micelle forming systems, it is suggested that a solvent that is effectively neutral (favours both blocks) is required as this negates micelle formation. The Hildebrand solubility parameter can be used to indicate the similarity of the solvent to a polymer and, hence, solubility.[46] However, for the PS-*block*-P4VP system, this approach is somewhat over simple since P4VP has considerable polarity. In this case, the Hansen solubility parameters are more useful providing estimates of individual contributions for dispersive (van der Waals), polar and hydrogen bonding.[47] Table 2 lists known Hansen solubility parameters for the materials used here. Toluene is poor solvent for the P4VP block because of its low polarity but a reasonable solvent for PS, THF is a good solvent for the P4VP block because of the good match with both its polarity and hydrogen bonding. Overall, it could be argued, that THF appears to be a better solvent for the BCP than toluene alone (since it has a reasonably similar dispersion component to PS as well as a polar component for THF) and hence it was used as the primary component in the casting solutions described above.

Table 2. Hansen Solubility Parameters ($MPa^{1/2}$ for Relevant Materials)

Material	Dispersion	Polarity	Hydrogen
Toluene	18.0	1.4	2.0
THF	16.8	5.7	8.0
Ethanol	15.8	8.8	19.4

PS			18.6	0.2	0.0
P4VP			18.1	6.8	7.2
PS-*b*-P4VP	19.3	5.9	0.9		

Note to table: Hansen Solubility Parameters were taken from various sources.[48-50]

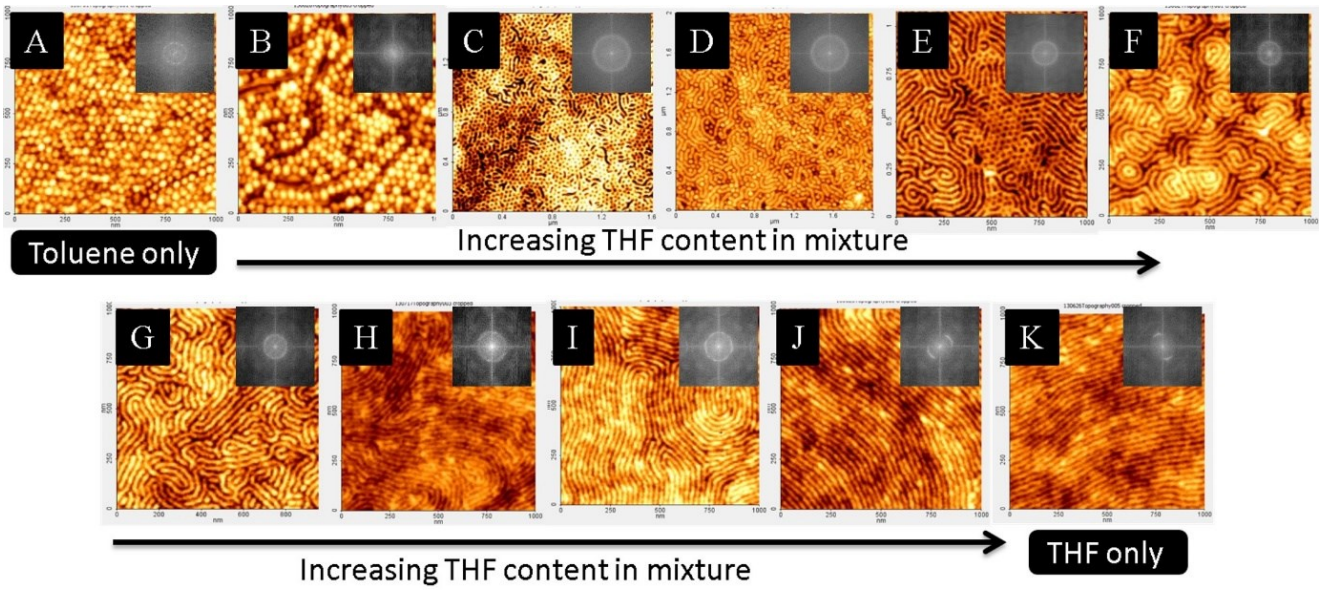


Fig. 2 Topographic AFM images (1x1µm) of PS_{9k}-*block*-$P4VP_{9.2k}$ copolymer cast from toluene/THF (80/20) and solvent annealed at 50 °C for 4h in different saturated solvent vapour environments of: (A) pure toluene, (B) toluene/THF =90/10, (C) toluene/THF =80/20, (D) toluene/THF =70/30, (E) toluene/THF =60/40, (F) toluene/THF =50/50, (G) toluene/THF =40/60, (H) toluene/THF =30/70, (I) toluene/THF =20/80, (J) toluene/THF =10/90 and (K) pure THF. All solvent compositions are given as (v/v). FFT patterns inset show the difference in the degree of order.

The more neutral nature of THF can be verified by the AFM data presented in Fig. 2 where the results of solvent annealing a PS_{9k}-*block*-$P4VP_{9.2k}$ copolymer in various toluene/THF mixtures (50 °C, 4 h). In Figs. 2 (A-K), there is a distinct change of morphology from micelle structures to well-defined microphase separated arrangements. For convenience, the solvent vapour

annealing (SVA) conditions can be divided into three distinct regions: (I) SVA in pure toluene, (II) SVA in toluene rich mixture of toluene/THF and (III) SVA in a THF rich mixture.

SVA in pure toluene (Fig. (2A))

As postulated earlier, solvent annealing in toluene is ineffective in altering the morphology of the as-cast films from their micelle type structure because it is a poor solvent for the P4VP block. The mean spacing for both as-cast and solvent annealed micelles remains unchanged as measured by AFM (~28 nm). Clearly, the BCP forms a P4VP rich core and a PS corona because of the favourable interactions of the polymer for the PS block. Even extended annealing periods of 24 h had no measurable effect on film morphology. It should be noted that whilst the morphology is largely unaltered, changes in the order of the micelle arrangement can be seen with significantly greater order after solvent annealing. Larger areas of a well-defined hexagonal arrangement can be seen compared to the image in Figure 1(A). This is evidenced by the changes in the FFT (Fast Fourier Transform) data.

SVA in a toluene rich mixture of toluene/THF (Fig. 2(B-F))

The addition of even small amounts of THF to toluene, for the solvent annealing procedure had a noticeable effect on the morphology. A 90:10 v/v mixture did not alter the morphology but changes in spacing and apparent feature size can be seen with increase in micellar size to around 29 nm consistent with some swelling of the P4VP core by the addition of THF. Note that although the swelling is not directly observed its effect is seen by inclusion of free volume caused by rapid solvent loss during removal from the chamber. Further addition of THF (80/20 v/v, Figure 2(C) begins to transform the micelle structure into a structure suggestive of a microphase separated arrangement with a change in height variation across the substrate decreasing from 5-6 nm for micelle structures to 2-3 nm for the phase separated like patterns.

The image seen in Figure 2(C) is more complex than might be imagined since both lines and cylinder or sphere arrangements can be seen. It seems unlikely that enough solvent swelling is seen to result in a gross composition change to form either cylinder of spherical microphase separated structures. In AFM, the lighter regions of the image are due to the P4VP block and it would appear that this initial structure represents a transition between a micelle arrangement and a microphase separated structure and might be a type of perforated lamellar structure with PS lamellae changing orientation so as to emerge from the surface.[51-53] At compositions of 70/30 and 60/40 v/v (Figure 2(D) and 2(E), the structure becomes more regular with regions of a lamellar-like pattern emerging together with remnants of the hexagonal spherical/cylinder arrangement. At a 50/50 v/v ratio of toluene/THF (Figure 2(F)), the lamellar phase extends across the entire substrate and any 'dot' like structures can be described as defects within the gross morphology. It is also worth stressing that in these studies we saw no evidence of a microphase separated lamellar structure oriented parallel to the surface plane. This suggests that the use of the THF as a co-solvent in the anneal process provides a 'neutral' interface that promotes vertical orientation of the lamellae.

SVA in THF rich mixture (Fig. 2(G-K))

Between 50% and 100% v/v THF the lamellar arrangement is maintained. The only noticeable visual change is an increase of the persistence length of the aligned domains and an increase in 'grain size'. At 90% and 100% THF, the persistence length exceeds 100 nm. The reason for well-ordered nature of the system clearly relates to the neutrality of the THF solvent which lowers the interactions between the PS and P4VP by effectively separating blocks and increasing chain mobility, allowing defect annihilation.[25] This would contrast a more block selective system since this would primarily result in selective block swelling whilst maintaining block-to-

block interfaces. The domain-to-domain spacing was estimated at 25 nm. In the AFM images, almost equal diameters the lighter P4VP block and the darker PS block confirms the lamellar structure of the BCP. Noticeable change in the FFT patterns also supports the hypothesis. This is significantly lower than for spacings observed with toluene rich SVA and this is consistent with reduced THF swelling of the PS component compared to toluene as suggested by the data in Table 2. It, thus, appears that THF is an 'ideal' annealing solvent for this PS-*block*-P4VP copolymer.

Table 3: The film thicknesses of PS_{20k}-*block*-$P4VP_{17k}$ and PS_{9k}-*block*-$P4VP_{9.2k}$ copolymer thin films casted from toluene/THF (80/20) solvent annealed at 50 ^{o}C for different time and different solvent vapour environment

BCP	Annealing solvent/s	Annealing time	Thickness (nm)
PS_{9k}-*block*-$P4VP_{9.2k}$	toluene/THF =80/20	0	26
PS_{9k}-*block*-$P4VP_{9.2k}$	Toluene	4 h	27 ± 1
PS_{9k}-*block*-$P4VP_{9.2k}$	toluene/THF =90/10	4 h	27 ± 1
PS_{9k}-*block*-$P4VP_{9.2k}$	toluene/THF =80/20	4 h	27 ± 2
PS_{9k}-*block*-$P4VP_{9.2k}$	toluene/THF =70/30	4 h	28 ± 2
PS_{9k}-*block*-$P4VP_{9.2k}$	toluene/THF =60/40	4 h	29 ± 3
PS_{9k}-*block*-$P4VP_{9.2k}$	toluene/THF =50/50	4 h	28 ± 2
PS_{9k}-*block*-$P4VP_{9.2k}$	toluene/THF =40/60	4 h	28 ± 2
PS_{9k}-*block*-$P4VP_{9.2k}$	toluene/THF =30/70	4 h	29 ± 1
PS_{9k}-*block*-$P4VP_{9.2k}$	toluene/THF =20/80	4 h	29 ± 1
PS_{9k}-*block*-$P4VP_{9.2k}$	toluene/THF =10/90	4 h	30
PS_{9k}-*block*-$P4VP_{9.2k}$	THF	4 h	30
PS_{20k}-*block*-$P4VP_{17k}$	toluene/THF =80/20,	As-spun	28
PS_{20k}-*block*-$P4VP_{17k}$	THF	30 min	29 ± 1
PS_{20k}-*block*-$P4VP_{17k}$	THF	1 h	30 ± 1
PS_{20k}-*block*-$P4VP_{17k}$	THF	2 h	30 ± 1
PS_{20k}-*block*-$P4VP_{17k}$	THF	3 h	31
PS_{20k}-*block*-$P4VP_{17k}$	THF	6 h	31

It should also be noted that both the kinetics of phase separation and the equilibrium structure are modified by solvents because of the effective vapour pressures during solvent annealing. It is important to note that at 50 ^{o}C these two solvents have quite different saturated vapour pressures

with measured values of 12.5 kPa and 58 kPa for toluene and THF respectively. Since this is an ideal solution, Raoult's law[54] is obeyed and can be used to sketch the expected vapour pressure through the composition range (Fig. 3(A)) and the amount of THF in the vapour phase (Fig. 3(B)). As can be seen, increased THF content results in increased vapour pressure of THF compared to toluene. One manifestation of this is seen in increasing thickness of the films as measured by ellipsometery. As cast films and toluene annealed films have a measured thickness of 26 nm but as the THF content increases, the film thickness increases to 30 nm. Table 3 summarizes the film thicknesses of PS_{9k}-*block*-$P4VP_{9.2k}$ copolymer thin films casted from toluene/THF (80/20) solvent annealed at 50 ^{o}C for 4h in different saturated solvent vapour environment as measured by ellipsometry and the variation of film thicknesses throughout the substrate was estimated by the AFM images. It is suggested this is because of increased swelling during solvent annealing followed by rapid de-swelling of the films on exposure to atmosphere. These results in increased (trapped) free volume as the film becomes kinetically 'frozen' and a higher film thickness compared to less swollen films.

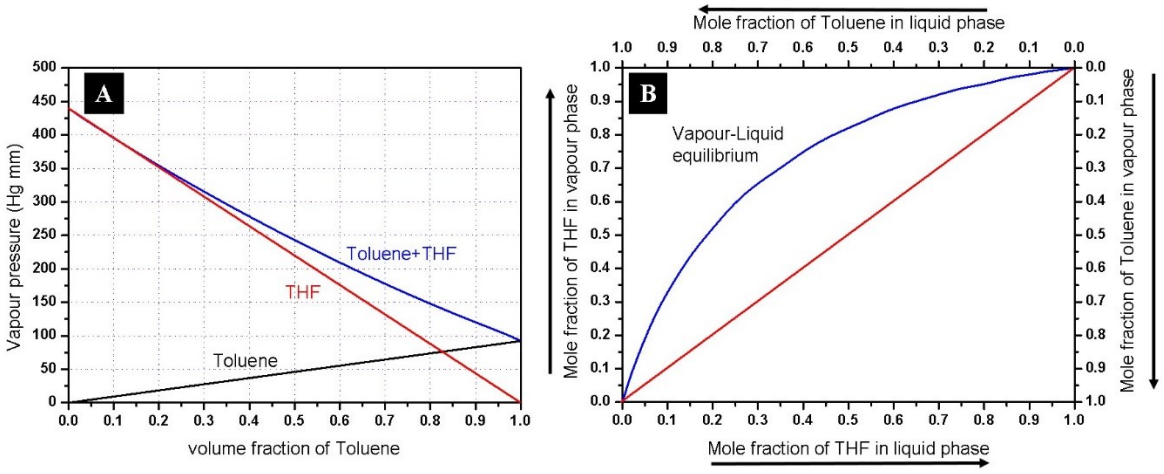


Fig. 3 (A) The vapour pressures of a solution of the two liquids, toluene and THF at 50 ^{o}C, is the sum of the two individual vapour pressures, calculated by Raoult's law. (B) Vapour-Liquid equilibrium diagram of toluene and THF mixture.

The data in Fig. 3 also helps to explain the variation in morphology observed across the whole concentration range because even at low THF liquid content, the vapour is highly enriched in THF. This explains the dramatic change in morphology at low THF content and the consistency (little change with toluene content) of the morphological data at higher THF content (Fig. 2). Similar dependence on composition was seen for the larger molecular weight PS_{20k}-*b*-$P4VP_{17k}$ system but is not reported here for brevity.

It is also important to explore the kinetics of the SVA process. Similar results were seen for both the BCPs and data shown in Fig. 4 of the PS_{20k}-*block*-$P4VP_{17k}$ copolymer are indicative of the microphase separation of both systems. Fig. 4 describes the effects of SVA time of thin films spin-coated from 0.5 wt% toluene/THF (80/20) solutions of PS_{20k}-*block*-$P4VP_{17k}$ copolymer and solvent annealed in THF. As-cast film thickness was 28 nm measured by ellipsometery and had the expected dried micellar structure (Fig. 4(A)). After a SVA period of 30 minutes (Fig. 4(B)), it is clear that the swelling of the films leads to merging of the P4VP cores and the formation of elongated micelle structures. Note that the size of the spherical micelles in Fig. 4(A) is 35 nm by AFM and where visible in Fig. 4(B) are generally about half the diameter of similar structures seen after extended solvent annealing and the elongated micelles seen in Fig. 4(B). Note, however that a few more swollen spherical structures can also be seen. The data suggest that at the lower SVA times that the film is not completely swollen by the THF and that Fig. 4B represents a rearrangement sponsored by the swelling. Note that it is assumed the swollen morphology is maintained due to freezing-in of the structure during rapid solvent evaporation.

After a solvent annealing time of 1 h (Fig. 4(C)), the micelle type structure has transitioned to a distinct lamellar microphase separated pattern across most of the substrate with only isolated regions of dot like structures. This phase transition is likely related to the degree of swelling. At low swelling, short SVA times; micelles survive (from spin-coating) because chain mobility is low. As the initial time increases, solvent swelling increases causing chain mobility and attaining the equilibrium phase-separated structure. With further increase in solvent annealing time (Figs. 4(D-F)), the film becomes flat with increasing order and lower defectivity. The thickness of the solvent annealed film after 6 h is measured at 31 nm (Table 3) consistent with an increased free volume as seen above. The domain spacing is 35 nm as measured by AFM. Note that these films are significantly less well ordered than those formed by similar treatment of the lower molecular weight PS-*block*-P4VP copolymer (compare Fig. 4(F)) and Fig. 2(K). This is thought to be because of diffusion limitations of the longer chains.

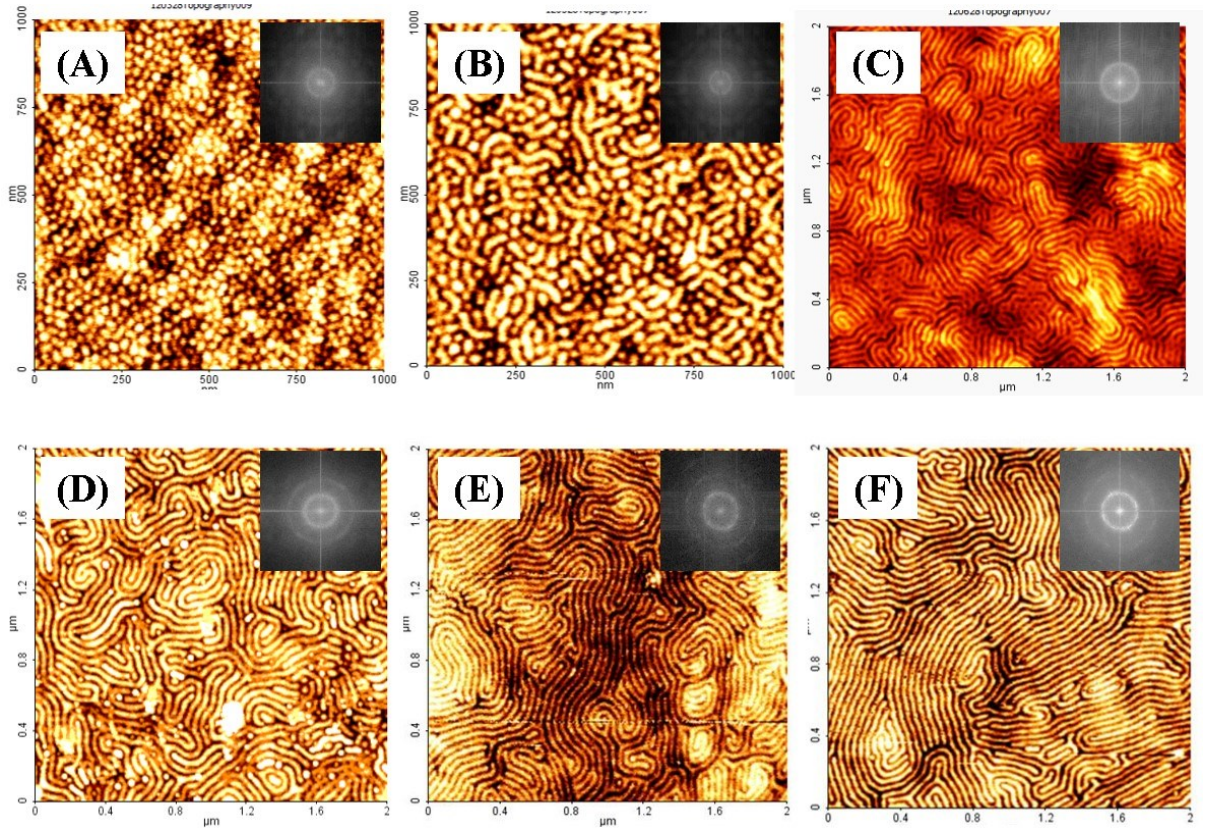


Fig. 4 AFM images of PS_{20k}-*block*-$P4VP_{17k}$ copolymer thin film casted from toluene/THF (80/20) (A) as-spun and solvent annealed at 50 ^{o}C for different time in THF vapour for (B) 30 min, (C) 1 h, (D) 2 h, (E) 3 h and (F) 6 h. FFT patterns inset show the difference in the degree of order.

BCP reconstruction with ethanol

PS-*block*-P4VP copolymer films are often subject to ethanol treatment to cause 'reconstruction'. This process is used to enhance the etching contrast between both PS and P4VP blocks as well providing a template for insertion of metal ions into the P4VP block [55]. Ethanol is a non-acidic polar solvent which selectively swells the P4VP block (Table 2). The pyridine groups present in P4VP are non-ionized and can interact with ethanol via hydrogen bonding. Due to the weak hydrogen bonding it is not expected that the P4VP block is chemically decomposed or removed from the BCP (since the covalent bond strength is high) but is more likely to swell and provide larger feature sizes than the lamella formed after solvent annealing. As shown in Fig. 5, a number of 3 h solvent annealed microphase separated PS_{9k}-*block*-$P4VP_{9.2k}$ copolymer thin film are reconstructed by immersing them in anhydrous ethanol for different times (between 2 and 20 min) to study the swelling (and/or solubility) behaviour of the P4VP block. When the PS_{9k}-*block*-$P4VP_{9.2k}$ copolymer film is immersed in ethanol for 2 min (Fig. 5A) followed by drying under nitrogen gas, the P4VP domains become partially swollen and the centre-to-centre distance between lamella is increased from 25 to 26 nm, by AFM, compared to a PS_{9k}-*block*-$P4VP_{9.2k}$ copolymer thin film which did not receive an ethanol exposure. During further reconstruction (in ethanol) for times between 5 and 20 min (Figs. 5(B-E)) the P4VP chains further swell to 30 nm (lamellae spacing). Ethanol exposure also results in the increase in the thickness of the films (~30 nm for the phase separated film) as measured by ellipsometry.[55]

The height profile can also be measured by AFM. Table 4 summarizes the film thickness and height profile of the swollen films for different time. The swollen of the P4VP domain further confirmed by the cross-sectional TEM image for the BCP film reconstructed for 7 min (inset of Fig. 5C). The measured lamellar spacing is ~ 30 nm whereas the film thickness associated to the P4VP domain changes from 30 nm to 32 nm. The PS blocks remained unchanged upon exposure to ethanol. The periodicity (~ 15 nm half pitch) of the wavy nature of the film surface confirms the lamellar phase of the PS_{9k}-*block*-$P4VP_{9.2k}$ copolymer film. It is also clear that at these extended exposures ethanol sufficiently swells P4VP domain and can lead to local areas of the pattern where the structure is damaged (black areas in the AFM images). The damage appears to relate to some dissolution of chains and probably results from the swollen chains weakening the polymer-substrate attachment (delamination) As exposure increases and particularly at a longer swelling time (~20 min or more), due to high degree of swelling, the surface of the BCP layer became increasingly rough as significant material is delaminated.

Table 4: Film thicknesses of PS_{9k}-*block*-$P4VP_{9.2k}$ copolymer films after ethanol reconstruction for different times.

Ethanol exposure time (min)	Film thickness (nm)
2	30
5	31 ± 1
7	32 ± 1
10	32 ± 2
20	33 ± 3

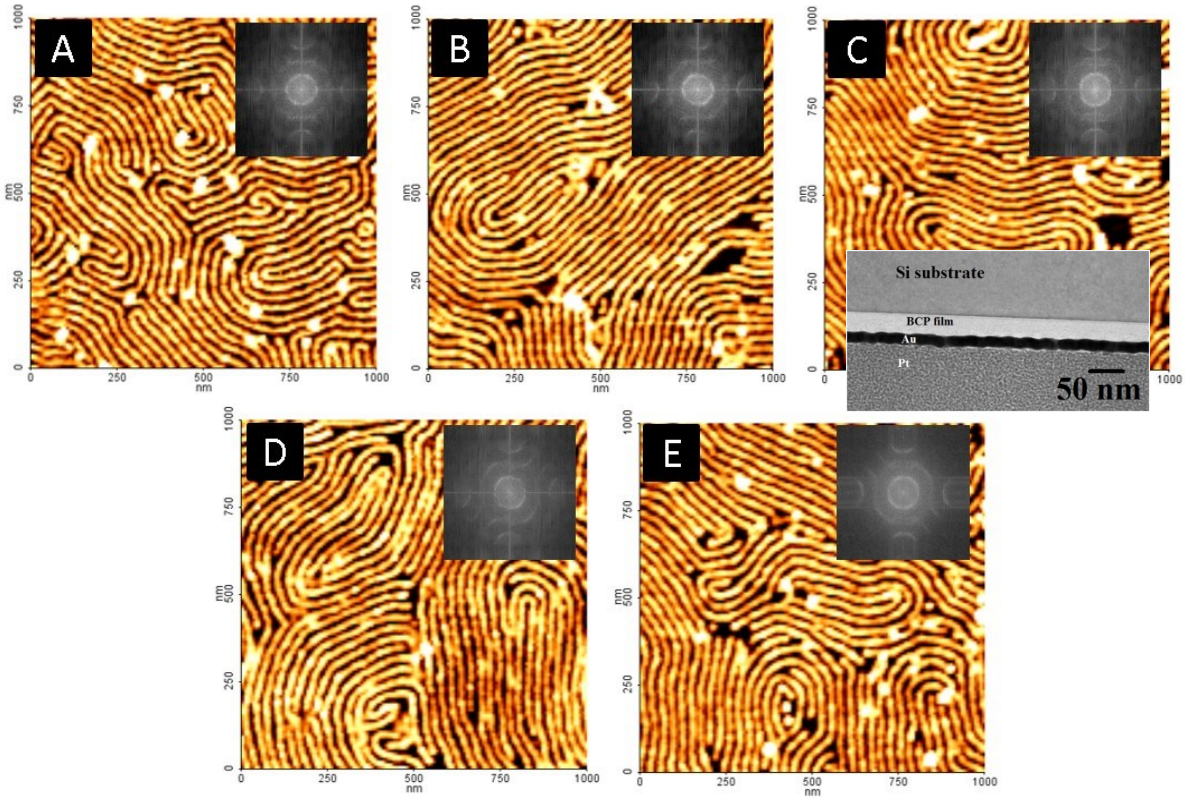


Fig. 5 Topographic AFM images (1 um x 1 um) of reconstructed PS_{9k}-*block*-$P4VP_{9.2k}$ copolymer thin films for different time (A) 2min, (B) 5min, (C) 7min, (D) 10min and (E) 20min respectively. FFT patterns (inset) show the difference in the degree of order. Inset of (C) shows corresponding cross-sectional TEM image.

Formation of molybdenum oxide and sulphide nanowire arrays:

The microphase separated PS_{20k}-*block*-$P4VP_{17k}$ copolymer thin films were used to fabricate molybdenum oxide and then sulphide nanowire arrays. This confirmed the morphology of the systems as simple lamellar structures. For this, molybdenum (V) chloride solution of 0.5 wt% was prepared in ethanol and spin coated onto the phase separated film at 3000 rpm for 30s followed by UV/Ozone treatment to oxidize the precursor and remove the polymer.[59] Fig. 6a shows the MoO_3 nanowire formed with a pitch size of 37 nm. These nanowires were subjected to sulphurization at a temperature of 300^{o}C for 30 min to form MoS_2 nanowires on substrate

surface. Fig. 6b shows identical ordered continuous MoS_2 nanowire arrays of diameter of ~25 nm. This confirms the successful application of the formation of inorganic nanostructures using the microphase separated lamellar forming PS_{20k}-*block*-$P4VP_{17k}$ copolymer thin films.

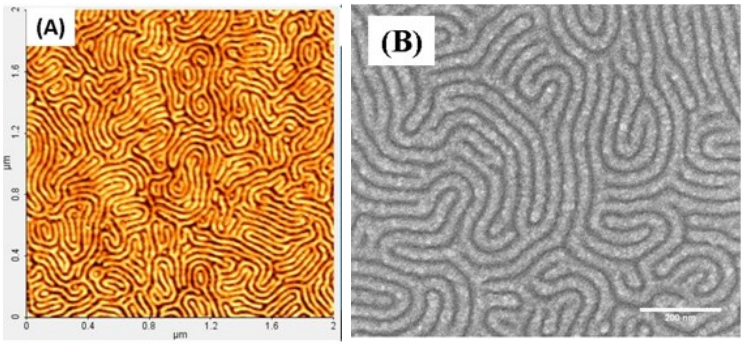


Fig. 6 Topographic AFM and SEM images of MoO_3 and MoS_2 nanowire arrays using PS_{20k}-*block*-$P4VP_{17k}$ copolymer thin films respectively.

Discussion and Conclusions

In this work it was found that extended SVA of micellar PS-*block*-P4VP copolymer films in THF vapour results in well-defined microphase separated structures. This work contrasts dramatically with previous work by Kim et al.[56] who have reported that when toluene cast PS-*block*-P4VP copolymer thin films containing micelles are solvent annealed in THF there are morphological changes but micelle structures persist. Our observations are consistent with the THF being a good solvent for the BCP and somewhat neutral in its interactions with both blocks. The agreement of the phase behaviour and the THF Hansen solubility parameters with those of PS-*block*-P4VP copolymer is consistent with this mechanism. It must be stressed that PS-*block*-P4VP copolymer Hansen parameters are not well-established and over analysis is possible. There is generally a paucity of high quality data on both solvent parameters and interaction parameters for these PS-*block*-P4VP copolymer systems (as well as other BCPs) despite the considerable research work in this area.

One of the main differences in the work of Kim et al[56] and here is the solvent annealing temperature (25 ^{o}C and 50 ^{o}C respectively) and differences may be explained by variation of these terms with temperature. However we can conclude that THF solvent annealing can be used to generate well-defined arrangements of PS-*block*-P4VP copolymer lamellar structures and ordain long range order and vertical orientation of the lamellae to the surface plane. For these high-χ systems, it does appear that solvent annealing in neutral solvents is important in generating well-defined arrangements. The method is robust and reliable and offers a simple means to generate these structures with possibly important applications of device fabrication. Cylinder forming PS-*block*-P4VP copolymer has been shown to be applicable in this area[55, 57-58] but lamellar systems have advantages compared to cylindrical structures.[28] Recently, we have shown the use of this block copolymer system in fabrication of two-dimension molybdenum disulfide (2D MoS_2) by simple process.[59]

Acknowledgements

The authors would like to thank Science Foundation Ireland for support of this project through Semiconductor Research Corporation 2013-OJ-2444 grant, 09/SIRG/I1621 grant.

Notes and References

1 F. S. Bates and G. H. Fredrickson, *Annual Review of Physical Chemistry* 1990, **41**, 525.

2 J. Chai, D. Wang, X. Fan and J. M. Buriak, *Nat Nano* 2007, **2**, 500.

3 T. Ghoshal, R. Senthamaraikannan, M. T. Shaw, J. D. Holmes and M. A. Morris, *Nanoscale* 2012, **4**, 7743.

4 X. Gu, P. Dorsey and T. P. Russell, *Advanced Materials* 2012, **24**, 5505.

5 D. H. Kim, X. Jia, Z. Lin, K. W. Guarini and T. P. Russell, *Advanced Materials* 2004, **16**, 702.

6 D. H. Kim, S. H. Kim, K. Lavery and T. P. Russell, *Nano Letters* 2004, **4**, 1841.

7 D. H. Kim, Z. Sun, T. P. Russell, W. Knoll and J. S. Gutmann, *Advanced Functional Materials* 2005, **15**, 1160.

8 X. Li, K. H. A. Lau, D. H. Kim and W. Knoll, *Langmuir* 2005, **21**, 5212.

9 J. P. Spatz, S. Mössmer, C. Hartmann, M. Möller, T. Herzog, M. Krieger, H.-G. Boyen, P. Ziemann and B. Kabius, *Langmuir* 2000, **16**, 407.

10 J. Xu, S. W. Hong, W. Gu, K. Y. Lee, D. S. Kuo, S. Xiao and T. P. Russell, *Advanced Materials* 2011, **23**, 5755.

11 R. Farrell, T. Fitzgerald, D. Borah, J. Holmes and M. Morris, *International Journal of Molecular Sciences* 2009, **10**, 3671.

12 D. J. C. Herr, *Journal of Materials Research* 2011, **26**, 122.

13 H.-C. Kim, S.-M. Park and W. D. Hinsberg, *Chemical Reviews* 2010, **110**, 146.

14 T. P. Lodge and M. C. Dalvi, *Physical Review Letters* 1995, **75**, 657.

15 L. Leibler, *Macromolecules* 1980, **13**, 1602.

16 S. O'Driscoll, G. Demirel, R. A. Farrell, T. G. Fitzgerald, C. O'Mahony, J. D. Holmes and M. A. Morris, *Polymers for Advanced Technologies* 2011, **22**, 915.

17 X. Shuaigang, Y. XiaoMin, W. E. Erik, L. Young-Hye and F. N. Paul, *Nanotechnology* 2005, **16**, S324.

18 H.-C. Kim and T. P. Russell, *Journal of Polymer Science Part B: Polymer Physics* 2001, **39**, 663.

19 Z. Di, D. Posselt, D.-M. Smilgies and C. M. Papadakis, *Macromolecules* 2010, **43**, 418.

20 Y. Xuan, J. Peng, L. Cui, H. Wang, B. Li and Y. Han, *Macromolecules* 2004, **37**, 7301.

21 K. W. Gotrik and C. A. Ross, *Nano Letters* 2013, **13**, 5117.

22 J. Peng, D. H. Kim, W. Knoll, Y. Xuan, B. Li and Y. Han, *The Journal of Chemical Physics* 2006, **125**, 064702.

23 T. P. Lodge, B. Pudil and K. J. Hanley, *Macromolecules* 2002, **35**, 4707.

24 S. Niu and R. F. Saraf, *Macromolecules* 2003, **36**, 2428.

25 C. Sinturel, M. Vayer, M. Morris and M. A. Hillmyer, *Macromolecules* 2013, **46**, 5399.

26 J. Bang, U. Jeong, D. Y. Ryu, T. P. Russell and C. J. Hawker, *Advanced Materials* 2009, **21**, 4769.

27 M. A. Morris, *Microelectronic Engineering* 2015, **132**, 207.

28 M. P. Stoykovich and P. F. Nealey, *Materials Today* 2006, **9**, 20.

29 E. W. Edwards, M. P. Stoykovich, M. Müller, H. H. Solak, J. J. de Pablo and P. F. Nealey, *Journal of Polymer Science Part B: Polymer Physics* 2005, **43**, 3444.

30 D. Borah, S. Rasappa, R. Senthamaraikannan, B. Kosmala, M. T. Shaw, J. D. Holmes and M. A. Morris, *ACS Applied Materials & Interfaces* 2013, **5**, 88.

31 G. Kim and M. Libera, *Macromolecules* 1998, **31**, 2569.

32 W. J. Durand, G. Blachut, M. J. Maher, S. Sirard, S. Tein, M. C. Carlson, Y. Asano, S. X. Zhou, A. P. Lane, C. M. Bates, C. J. Ellison and C. G. Willson, *Journal of Polymer Science Part A: Polymer Chemistry* 2015, **53**, 344.

33 W. Zha, C. D. Han, D. H. Lee, S. H. Han, J. K. Kim, J. H. Kang and C. Park, *Macromolecules* 2007, **40**, 2109.

34 T. Nose, *Polymer* 1995, **36**, 2243.

35 T. L. Bucholz and Y.-L. Loo, *Macromolecules* 2006, **39**, 6075.

36 M. R. Hammond, E. Cochran, G. H. Fredrickson and E. J. Kramer, *Macromolecules* 2005, **38**, 6575.

37 H. Frielinghaus, N. Hermsdorf, K. Almdal, K. Mortensen, L. Messé, L. Corvazier, J. P. A. Fairclough, A. J. Ryan, P. D. Olmsted and I. W. Hamley, *Europhys. Lett.* 2001, **53**, 680.

38 N. Torikai, I. Noda, A. Karim, S. K. Satija, C. C. Han, Y. Matsushita and T. Kawakatsu, *Macromolecules* 1997, **30**, 2907.

39 S.-Y. Park, W.-H. Sul and Y.-J. Chang, *Macromolecules* 2007, **40**, 3757.

40 J. Kim, J. Lee and D. Lee, *Macromol. Res.* 2008, **16**, 267.

41 G. Roman, M. Martin and P. S. Joachim, *Nanotechnology* 2003, **14**, 1153.

42 S.-H. Yun, S. I. Yoo, J. C. Jung, W.-C. Zin and B.-H. Sohn, *Chemistry of Materials* 2006, **18**, 5646.

43 J. F. Tassin, R. L. Siemens, W. T. Tang, G. Hadziioannou, J. D. Swalen and B. A. Smith, *The Journal of Physical Chemistry* 1989, **93**, 2106.

44 M. Aizawa and J. M. Buriak, *Journal of the American Chemical Society* 2005, **127**, 8932.

45 C.-Y. Chang, Y.-C. Lee, P.-J. Wu, J.-Y. Liou, Y.-S. Sun and B.-T. Ko, *Langmuir* 2011, **27**, 14545.

46 E. H. I. J. Brandrup, E.A. Grulke *Polymer handbook 1. 1*. Wiley: Hoboken, NJ, 1999.

47 C. M. Hansen, Solubility Parameters - An Introduction. In *Hansen Solubility Parameters*, CRC Press: 1999.

48 E. Manias and L. Utracki, Thermodynamics of Polymer Blends. In *Polymer Blends Handbook*, Utracki, L. A.; Wilkie, C. A., Eds. Springer Netherlands: 2014; pp 171.

49 L. A. Utracki, Introduction to Polymer Blends. In *Polymer Blends Handbook*, Utracki, L. A., Ed. Springer Netherlands: 2003; pp 1.

50 C. M. Hansen and A. L. Smith, *Carbon* 2004, **42**, 1591.

51 I. Park, S. Park, H.-W. Park, T. Chang, H. Yang and C. Y. Ryu, *Macromolecules* 2006, **39**, 315.

52 Y. Yin, P. Sun, R. Jiang, B. Li, T. Chen, Q. Jin, D. Ding and A.-C. Shi, *The Journal of Chemical Physics* 2006, **124**, 184708.

53 L. Tsarkova, A. Knoll, G. Krausch and R. Magerle, *Macromolecules* 2006, **39**, 3608.

54 R. W. Kugel, *Journal of Chemical Education* 1998, **75**, 1125.

55 C. Cummins, D. Borah, S. Rasappa, A. Chaudhari, T. Ghoshal, B. M. D. O'Driscoll, P. Carolan, N. Petkov, J. D. Holmes and M. A. Morris, *Journal of Materials Chemistry C* 2013, **1**, 7941.

56 T. H. Kim, J. Huh, J. Hwang, H.-C. Kim, S. H. Kim, B.-H. Sohn and C. Park, *Macromolecules* 2009, **42**, 6688.

57 C. Cummins, A. Gangnaik, R. A. Kelly, D. Borah, J. O'Connell, N. Petkov, Y. M. Georgiev, J. D. Holmes and M. A. Morris, *Nanoscale* 2015, **7**, 6712.

58 C. Cummins, R. A. Kelly, A. Gangnaik, Y. M. Georgiev, N. Petkov, J. D. Holmes and M. A. Morris, *Macromolecular Rapid Communications* 2015, **36**, 762.

59 A. Chaudhari, T. Ghoshal, M. T. Shaw, J. O'Connell, R. A. Kelly, C. Glynn, C. O'Dwyer, J. D. Holmes, M. A. Morris, Adv. Mater. Inter. 2016, 1500596.